

# Optimal design of fossil-solar hybrid thermal desalination for saline agricultural drainage water reuse



Matthew D. Stuber

WaterFX, Inc., PO Box 2304, Healdsburg, CA 95448, USA

## ARTICLE INFO

### Article history:

Received 28 July 2015

Received in revised form

1 December 2015

Accepted 7 December 2015

Available online 24 December 2015

### Keywords:

Parabolic trough

Solar desalination

MED

Water reuse

Robust optimization

## ABSTRACT

Ultra-high recovery solar thermal desalination of agricultural drainage water is presented as one solution to the historic extreme drought and long-standing salt accumulation problems facing California's fertile Central Valley region. Building on the results obtained from a recent pilot demonstration of a novel solar thermal desalination system, a techno-economic analysis is presented using an existing agricultural region as a case study. Three strategies are considered: continue retiring farmland as crop productivity wanes in future years, desalinate saline drainage water with a novel distillation process using natural gas as the fuel source, and desalinate using natural gas and solar as a hybrid energy source. The study is cast as a parametric optimization problem taking into account natural gas costs and water purchase contract pricing. The results show that with projections of the long-term effects and cost of salt accumulation in the region, solar thermal desalination is economically favorable over both the alternative of doing nothing (retire farmland) as well as implementing conventional (non-renewable) thermal desalination. Most importantly, the results indicate that solar thermal desalination is an economically-viable solution that can increase the sustainability of farming in the region and create a new, sustainable, scalable source of additional freshwater.

© 2015 Elsevier Ltd. All rights reserved.

## 1. Introduction

### 1.1. Severe and persistent drought

The State of California (CA) is currently facing the worst drought in recorded history. Fig. 1 illustrates the severity of the widespread drought. A recent study using tree rings has concluded this drought is the worst in 1200 years [1]. This unfortunate conclusion was made in light of the findings that although reduced precipitation and high temperatures played an important role compounding the water deficit, they are not historically unprecedented [1]. In other words, California has a delicate water balance that is highly sensitive to perturbations from the norm. Researchers have concluded that global warming arising from human activity (greenhouse gas emissions) is further increasing the probability of conditions leading to the exceptional drought in California [2]. Hence, any proposed solution to water scarcity must also take into account greenhouse gas emissions.

Home to the largest and most productive agricultural region in the US, CA is arguably most affected by water scarcity in the

agriculture sector which accounts for nearly 80% of the total water-use in the state [3] (excluding environmental uses). This rich and fertile land of the Central Valley is responsible for supplying more than a third of the total US vegetables and nearly two-thirds of the total US fruits and nuts [4].

In 2014 alone, compounding effects resulted in a 6.6 million acer-ft (8.14 km<sup>3</sup>) reduction in surface water supply to the agriculture sector [6]. The 2014 drought would end up costing \$2.2B and 17,100 jobs in the agriculture sector [6] alone. Of the \$2.2B in losses, \$810M is from crop revenue losses. A recent report, citing real estate brokers in the region, disclosed that irrigated land in the Paso Robles, CA region was selling for \$15,000–\$20,000 per acre as opposed to just \$3000 per acre for dry land; with the disparity expected to get much worse as the drought continues [7]. The California Department of Food and Agriculture states that the average value of irrigated cropland is \$12,000/acre [4] illustrating the massive economic impact of drought on land value.

### 1.2. Salt accumulation and drainage

Water scarcity happens to be only one part of the problem negatively affecting the sustainability of California's agriculture

E-mail address: [stuber@alum.mit.edu](mailto:stuber@alum.mit.edu).

operations. The other part is the historic and long-standing issue of salt accumulation and impairment of arable land due to high water tables and poor drainage. In California's Central Valley, water is imported through the State and Federal Water Projects. The Tulare Lake and San Joaquin River Basins alone receive more than 1.8 million tonnes of salt annually through these water projects [8]. Researchers have estimated that since the completion of the Delta–Mendota Canal in 1951, more than 18 million tonnes of salt has been imported into the San Joaquin Valley [9]. The CA Department of Water Resources [10] estimates the net accumulation of salts in the San Joaquin Valley at 2.23 million tonnes annually. This salt import is estimated to contribute over 364 thousand tonnes of salt to the San Joaquin Basin confined aquifer among other untold impacts [8]. The salt import cannot be effectively managed at the source due to the extremely low concentrations (<500 ppm) of naturally occurring minerals. Further, the extraordinarily large volume makes treatment of the source prohibitively expensive.

Agricultural operations also intensify the salt accumulation problem as fertilizers and minerals are added for crop health. Salt accumulation in the region's soil and a shallow water table continue to drive agricultural productivity down as crop roots penetrate high-salinity stratification in the soil [8] and even forces growers to retire once-arable land. On the west side of the San Joaquin Valley, an estimated 379,000 acres, a very significant portion of the irrigated land, is impacted by drainage and salinity [8]. On the west side of the San Joaquin Valley, more than 113 thousand acres (45,700 ha) have already been retired due to salt accumulation and drainage problems [8]. It is expected that by 2030, the total land area affected by shallow saline groundwater is expected to grow by 12%–15% [11].

### 1.3. Desalination for drainage reuse: an in-valley solution

Desalination as a reuse strategy has the potential to increase the water-use efficiency of California's agricultural sector while providing a sustainable long-term in-Valley solution to drainage and salt accumulation in the Central Valley. The idea of desalinating saline drainage water is not necessarily novel and although a conventional approach would reduce the overall volume of drainage, without the proper technology and implementation, discharge of concentrated brine streams to the environment would still be an issue. Hence, the long-term success of any desalination approach to these problems hinges on sustainability. The benefits of desalinating saline drainage water over other reuse strategies, such as irrigating salt-tolerant crops, is that not only will it be recovering pure freshwater—which can be used for irrigating higher-value crops or transferred to municipal or other industrial users—but it will also be concentrating, isolating, and potentially sequestering the harmful salts. Since drainage is the product of irrigation activities, by recovering pure freshwater, the total water-use efficiency for irrigated crops is increased.

There are multiple technologies that can be used to desalinate water, in the general case; however, the quality of drainage water and other environmental conditions dramatically affect the technical viability of one solution over another. The feasibility of reverse-osmosis (RO) with respect to treating agricultural drainage in the San Joaquin Valley has been studied [12,13] and continues to be studied in an ongoing effort. One of the largest challenges facing RO is the reliability of the membranes for treating agricultural drainage water having high concentrations of sparingly-soluble salts, particulates, and organic matter [14]. Due to the nature of agricultural drainage water, the application of RO is limited as the chemical costs and energy costs are high. Further, the extent in which the drainage discharge volume can be reduced, which is quantified as the recovery, defined as

$$\% \text{ recovery} = \frac{\text{freshwater production rate}}{\text{saltwater feed rate}} \quad (1)$$

is limited due to membrane scaling and fouling. The limitation in recovery would require additional treatment, such as downstream forced-circulation thermal crystallization; which, on its own is extremely energy intensive. Lastly, emphasizing renewable energy when considering overall environmental impact, makes RO not a viable solution for desalination of agricultural drainage [15] on its own.

In 2013, researchers deployed a novel implementation of multi-effect distillation (MED) integrated with concentrated solar thermal power (CST), called a concentrated solar still (CSS), to treat agricultural drainage water at the Panoche Drainage District in the San Joaquin Valley [15]. The primary objective of the pilot project was the demonstration of high-recovery treatment and economic feasibility of the technology for this specific application, as well as the energy savings expected with the new technology [15]. However, an economic analysis of the technology implementation and value proposition were not discussed.

Advancements in solar thermal energy technologies are continuing to drive down investment costs, increase ease of deployment, and optimize direct coupling with process systems for process heat. In spite of this, applying CST in California for sustainable desalination at-scale is entirely novel. In this paper, the land-use efficiency and economics of deploying CSSs for agricultural drainage water reuse will be modeled and investigated by a case study of the agricultural region. The comparison will consider the option of deploying CSSs versus the alternative of retiring otherwise-fertile irrigable land which is currently considered an inevitability and part of the ongoing strategy [8,11,16–18]. Solar desalination as an in-Valley solution to drainage and salt accumulation enhances the sustainability of agribusiness in the Central Valley and helps secure the long-term success of one of the most important growing regions in the United States and the world.

## 2. Methods

Within drainage-impaired and salt impaired regions, fertile farmland is being transformed into drainage region and reuse region (growing lower-value salt-tolerant crops), as well as outright retired to control subsurface drainage and salts in order to keep adjacent farmland productive. This is not only a short-term solution since saltwater in the region will continue to accumulate, but it is also an inefficient use of fertile farmland [11]. It is proposed herein that a far more attractive alternative is to deploy CSSs to reduce the drainage region footprint and simultaneously generate revenue by producing freshwater and selling it to downstream municipal and industrial (M&I) users. Both fossil-fuel powered and solar thermal powered (with fossil-fuel backup) systems will be analyzed.

### 2.1. Solar resource

A solar array consisting of large parabolic trough solar concentrators (PTC), each with an aperture length of 6m and area of 656 m<sup>2</sup>, was modeled using recently published methods [19–21] including thermal storage based on the single-tank thermocline design. The model was simulated with data input for the typical meteorological year (TMY) from the NREL Solar Prospector [22] for the San Joaquin Valley site west of Fresno, CA. This data exists in the 8760 h/yr format and allows for dynamic modeling of the solar field over the entire year with hourly resolution. The model parameters used can be found in Appendix A as well as a monthly break-down of the solar irradiance data.

An emphasis on renewable energy will be studied by comparing an unconstrained case (i.e., allowing the solar array to be sized freely) to a constrained case where a constraint on the total allowed consumption of natural gas is imposed. Each solar technology has a varying packing density (i.e., the ratio of the total collector area to the total land requirement). The PTC technology will be assumed to have a packing density of 33% (for every  $\text{m}^2$  of collector aperture area, you need  $3 \text{ m}^2$  of land).

## 2.2. Water treatment

A modularized system with a daily production capacity of 1 million gallons ( $3.07 \text{ acre-ft}$ ,  $3,785 \text{ m}^3$ ) is considered. The specific thermal energy consumption is taken to be  $34.9 \text{ kWh/m}^3$  and the specific electrical energy consumption is taken to be  $1.5 \text{ kWh/m}^3$ , which is broken down as roughly  $1.3 \text{ kWh/m}^3$  for pumping and recirculating water (with  $1 \text{ kWh/m}^3$  for the MED alone) [15] and  $0.20 \text{ kWh/m}^3$  for circulating thermal oil (which is equal for both the fossil-only system and a solar-only system due to similar pressure drops). This system represents the commercial-scale version of the system recently piloted in the region by Stuber et al. [15]. The system consists of a 10-effect MED coupled to an advanced vapor-absorption heat pump for heat integration, and a fully integrated thermal crystallizer (with waste-heat recovery). Thermal energy will come from either a natural gas furnace, CST collectors and thermal storage for off-peak and nighttime operation, or some combination thereof.

## 2.3. Agricultural region

The agricultural land considered here is an existing agricultural region with drainage infrastructure and managed drainage “wetlands” region. The total land area is 97,000 acres ( $39,256 \text{ ha}$ ) including 6000 acres ( $2430 \text{ ha}$ ) of drainage wetlands. This means that there is 1 acre of drainage land (and reuse region) for every 15 acres of primary growing land. For comparison, in 2002 the wetlands accounted for just 2000 acres the region total. The drainage region receives roughly  $35,000 \text{ acre-ft/yr}$  ( $118,300 \text{ m}^3$ ) of water and about 65% of that is available for treatment. The remaining 35% is not available for treatment due to inefficiencies in the drainage infrastructure and liquid holdup in the land. It is assumed that some drainage region will need to be maintained due to these inefficiencies; which is taken as 2100 acres (35% of the original 6000 acres). The drainage water quality has been observed to vary dramatically throughout the year with salt concentrations as low as 6000 ppm total dissolved solids (TDS) and as high as 35,000 ppm TDS [15]. An average value of 15,000 ppm TDS is considered for modeling purposes. It is expected that between 10% and 30% of the growing region has been converted to drainage region or retired due to salt accumulation in the case of not implementing desalination [11]. The average conversion of 10% is considered for this study.

## 2.4. Financials

In 2013, this region had average crop revenues of  $\$2340/\text{acre}$ . An average profit margin on crops of 35% is considered, which is a bit more conservative than the USDA average of 40% [23]. The cost of capital will be 4% say by issuing bonds (the sensitivity of this number will be explored), inflation on food and energy prices is taken to be 3% and the capital discount rate is taken to be 4.5%. The project lifetime is taken to be 20y and the debt will be amortized over 10y. The debt occurs at Year 0 and water production (and

positive revenues) begin at Year 1. Over the 20y period, a linear retirement of growing region is realized up to the fraction discussed previously. Any freshwater produced from the CSS is transferred downstream to M&I users according to contract pricing. The pricing will be considered to grow at the rate of inflation. A range of Year 1 contract prices will be considered from  $\$1800/\text{acre-ft}$  to  $\$2200/\text{acre-ft}$  and each subsequent years costs will reflect an escalation due to inflation (pacing with rising energy costs). The cost basis for each water treatment module (not including solar) is  $\$8\text{M}$  and the cost basis for each PTC is roughly  $\$111,400$  (assuming volume pricing) with thermal storage costing  $\$20/\text{kWh}$  based on a single-tank thermocline design. The non-solar energy prices are taken to be  $\$0.10/\text{kWh}$  for electric and delivered natural gas prices are considered to range between  $\$6/\text{mmbtu}$  and  $\$9/\text{mmbtu}$  ( $\$20.47/\text{MWh}$  to  $\$30.71/\text{MWh}$ ).

## 2.5. Optimization

The optimal solar array sizing is highly dependent on the economics of the project. For example, one expects that as natural gas prices increase, solar would be a more favorable energy source. However, as the size of the solar array increases, the fraction of drainage region (or retired land) that is recovered for primary high-value growing region is reduced. In other words, increasing solar capacity benefits the project from both an environment perspective (reduced greenhouse gas emissions) and a finance perspective when natural gas costs are high; however, it also increases the land footprint of the project which offsets high-value cropland. Further, since high capital investment in the desalination equipment favors 24 h/day operation, there is an economic challenge in sufficiently over-sizing the solar system to ensure power production in worst-case conditions. For example, a design with 100% solar may be theoretically possible but it would require a massively over-sized solar array and storage system to ensure operation during the worst solar conditions (winter months) which would be prohibitively expensive. In fact, due to competing economic factors, it is not clear at this stage that without optimization, what fraction of solar (if any) should be favored due to its very high capital investment and footprint.

For discrete values of the M&I water contract price and Year 0 natural gas price (i.e., the gas price when the project construction begins) within the ranges considered above, the solar capacity (solar array size and storage capacity) will be optimized. Natural gas prices of  $C_{\text{gas}} \in [6, 9] \text{ \$/mmbtu}$  and M&I water contract prices of  $C_{\text{water}} \in [1800, 2200] \text{ \$/acre-ft}$  will be considered. Two cases for optimization will be considered. The first case will put no constraints on the fraction of energy that must come from solar (i.e., the unconstrained case). Conversely, the second case will require that at least 50% of the thermal energy must come from solar (i.e., the constrained case, an emphasis on renewables will be imposed). For each case, no economic value/cost will be placed on carbon emissions and no renewable energy credit or subsidy will be considered. This case accurately represents the current climate regarding non-standard (or even nonexistent) implementations of carbon cap-and-trade programs and renewable energy investment/financing programs.

The objective function for the optimization problems will be the net-present value (NPV) of the solar desalination project in the units of dollars per acre-ft of freshwater produced. The economic value of desalination is calculated by comparing the cash flows for the agribusiness adopting desalination with that of continuing with the current drainage strategy without desalination. The yearly profit (or loss) of the project is simply the difference between the

profit (or loss) from farming with desalination and without desalination and adding in the profit (or loss) from generating freshwater.

The optimization problem will seek to maximize the project's NPV while varying the solar array size (number of collectors) and thermal storage capacity (kWh of thermal energy). Due to the discrete nature of the model (e.g., only whole solar collectors can be used, hourly solar performance data, etc.), as well as the structure of the underlying equations, the optimization problem is nonlinear and nonsmooth. Examining the empirical data, nonsmoothness in solar field output arises, for example, due to local weather events (e.g., storm clouds) reducing the DNI to zero. This is especially problematic in low DNI winter months when the storage system may not be storing heat at all.

In order to solve the optimization problem, both genetic algorithms and the generalized reduced gradient method with multi-start will be employed along with thorough analysis. Alternatively, a smooth empirical model for the solar performance could be fit via parameter estimation and the problem could be formulated as a mixed-integer nonlinear program to be solved to global optimality. Also, an approach similar to [24] could be used in simulating and designing the field. However, what is expected to be gained by identifying a rigorous global optimal solution is potentially lost in the deviations of the empirical model from the data. It is expected that careful analysis of the problem and candidate solution(s) will provide a more accurate solution, from an annual operation perspective, for the specific region and application.

The formal statement of the optimal design problem is given in the following equation:

$$\begin{aligned} f_{\text{NPV}}^*(C_{\text{water}}, C_{\text{gas}}) &= \max_{N_s, H} f_{\text{NPV}}(N_s, H, C_{\text{water}}, C_{\text{gas}}) \\ \text{s.t. } N_s &\in \{n \in \mathbb{Z} : 13 \leq n \leq 52\} \\ H &\in \{h \in \mathbb{R} : 0 \leq h \leq 12\} \\ C_{\text{water}} &\in \{c \in \mathbb{R} : 1800 \leq c \leq 2200\} \\ C_{\text{gas}} &\in \{c \in \mathbb{R} : 6 \leq c \leq 9\} \end{aligned} \quad (2)$$

where  $f_{\text{NPV}} : \mathbb{Z} \times \mathbb{R} \times \mathbb{R} \times \mathbb{R} \rightarrow \mathbb{R}$  is the project NPV function, defined in the Appendix on the basis of per acre-ft of freshwater produced per year.

Solving (2) yields an optimal solution that is parameter dependent (i.e., dependent on the values of the water purchase price  $C_{\text{water}}$  and natural gas price  $C_{\text{gas}}$ ).

### 2.5.1. Robust design and worst-case feasibility

Since solving (2) yields an optimal solution that is parameter-dependent, there is an opportunity here to solve the feasibility problem (alternatively named the robust design problem). This problem is stated formally as the logical constraint:

$$\forall (C_{\text{water}}, C_{\text{gas}}) \in F_c \exists (N_s, H) \in F_d : f_{\text{NPV}} \geq 0 \quad (3)$$

where  $F_c \subset \mathbb{R} \times \mathbb{R}$  is the parameter (cost) interval taken as  $F_c = [6, 9] \times [1800, 2200]$  and  $F_d \subset \mathbb{Z} \times \mathbb{R}$  is the feasible design set. The feasibility/robust design problem (3) can be reformulated as the following min–max optimization problem:

$$\begin{aligned} \min_{C_{\text{water}}, C_{\text{gas}}} \max_{N_s, H} f_{\text{NPV}}(N_s, H, C_{\text{water}}, C_{\text{gas}}) \\ \text{s.t. } N_s &\in \{n \in \mathbb{Z} : 13 \leq n \leq 52\} \\ H &\in \{h \in \mathbb{R} : 0 \leq h \leq 12\} \\ C_{\text{water}} &\in \{c \in \mathbb{R} : 1800 \leq c \leq 2200\} \\ C_{\text{gas}} &\in \{c \in \mathbb{R} : 6 \leq c \leq 9\} \end{aligned} \quad (4)$$

This formulation has been used to address a number of diverse robust design problems from chemical process systems [25–29]

to weapon systems [30,31]. In Ref. [25], the feasibility problem (3) was reformulated as an equivalent max–min program which considered maximization over uncertain parameters and minimization over process controls. In that formulation, the performance and safety constraint was formulated as  $g \leq 0$  whereas the performance constraint here is formulated as  $g \geq 0$  and hence the equivalence. Further, in Ref. [25], the optimal design was considered in an outer program and hence fixed from the perspective of the feasibility constraint(s), which were expressed as the max–min inner program. The work of [26] takes this approach a step further by adding the additional question of just how large the uncertainty set can be for feasible operation. Ostrovsky et al. [27] developed weaker conditions for process feasibility as well as a new framework for solving the problem. The work of [28] and [29] extended the applicability of the process feasibility approach to a broader class of problems commonly encountered in process systems engineering applications. In Ref. [30] the authors presented one of the earliest algorithms for solving the feasibility problem making certain assumptions on the problem structure. Further, in Ref. [31] a general nonconvex algorithm for solving this problem is applied to the missile defense problem with explicit functions.

Contrasting the development presented herein with [25], in the latter formulation, the question being addressed is finding an optimal design such that for all realizations of uncertainty, there exist feasible control settings ensuring performance and safety of the process. Here the question being considered is not one of process feasibility (i.e., ensuring a feasible control setting for the worst-case realization of uncertainty) as the desalination process design is considered fixed and the uncertainty lies in the Year 0 gas price and water contract price; not influencing operation in the future. Hence, the relevant question being asked in (3) and (4) can be interpreted as: “faced with the worst-case economics at this stage, is there a design that is economically feasible?” which is equivalent to the logical constraint (3).

Solving this problem at the design stage is often important when a project is dependent on uncertain parameters, such as future energy costs. If the optimal solution value identified upon solving the program in (2) is nonnegative, the project is still economically favorable, even if the worst-case economics are realized. The solution will identify the worst-case design (i.e., the optimal design under the worst-case economic conditions) which will aid engineers and help guide investors assessing risk. It should be noted that without employing global optimization methods, a rigorous guarantee of feasibility cannot be obtained due to the nature of the problem. However, an analysis of this problem will still provide insight at this stage.

In order to solve the min–max problem in (2) it must first be reformulated as a semi-infinite program (SIP). The details of the reformulation follow from Stuber et al. [32]. After reformulating as an SIP, the algorithm of Mitsos [33] will be employed. The reformulation and the details of the algorithm can be found in Appendix A.2. The SIP subproblems are solved using both the generalized reduced gradient method employing a multi-start strategy as well as a genetic algorithm for comparison and analysis purposes. Since the problem is nonsmooth, thorough analysis is required to ensure that the optimization methods are returning relevant results since there is no guarantee for such problems. Further, it's worth reminding the reader that no rigorous guarantee of global optimality can be provided using these methods so an analysis of each subproblem is required. Upon solving each subproblem, an analysis of the solution obtained was performed to ensure that, if required, it was sufficiently close to a global optimum.

### 3. Results and discussion

#### 3.1. Optimization

In order to address the needs of the entire region considered (i.e., treat 22,750 acre-ft/yr of drainage), 20 modules will be required with a total capital cost of \$160M not including CST or thermal storage. For comparison, the Carlsbad, CA RO desalination facility for the San Diego County Water Authority has an expected cost of \$1B [34] for the equivalent capacity of 50 of the modules considered here. Not considering the economies of scale, the 20 module equivalent would have an expected cost of \$400M. Optimal sizing of the solar field was performed for four discrete values of  $C_{gas}$  and three discrete values of  $C_{water}$  and the economic results are shown in Fig. 2 through Fig. 4 for the case without constraints on the solar energy capacity (e.g., requirements to emphasize renewable energy).

The optimization results are fairly straight-forward. In every case, the NPV for the solar desalination project is greater than the NPV for the gas-only desalination project. Only in the case of \$2200/acre-ft contract pricing does the IRR favor the gas-only case for natural gas prices below \$7.50/mmbtu. However, from the perspective of the agribusiness, and its long-term success, the NPV is truly the stronger metric for performance here; which again, strongly favors the solar desalination project. There are some natural gas prices that push the gas-only desalination NPV negative for contract prices considered herein. Clearly, for these cases, the “doing nothing” approach (i.e., continue with the current drainage strategy without desalination) is favored over the gas-only desalination project. However, the solar desalination project is still favored over the “doing nothing” strategy.

In each of the results shown in Fig. 2 through Fig. 4, the NPVs and IRRs for the gas-only project show a dramatic reduction as the natural gas price goes from \$6/mmbtu to \$9/mmbtu. This is obviously expected since natural gas is the primary energy source in this case. However, it illustrates the sensitivity of the project’s economics to the price of natural gas, which can be quite volatile. The trends of the NPVs and IRRs for the solar project help illustrate how the reduced dependence on natural gas yields stronger economic results over the project lifetime despite the higher capital costs due to the solar equipment. It is worth noting that since the water contract price is only accounted for in the revenue calculation, and since both the solar and gas-only systems produce the same quantity of water, only the NPV varies between the different water contract values and not the optimal solutions themselves (i.e., the design). The optimal design for each gas price is shown in Table 1.

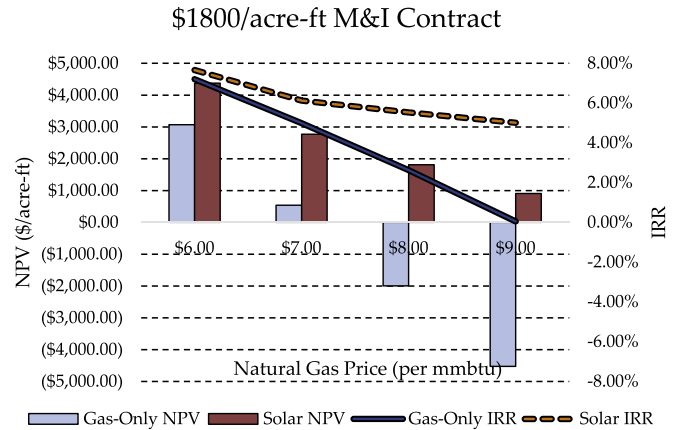


Fig. 2. The economic summary of the desalination projects with and without solar considering \$1800/acre-ft M&I water contract pricing at Year 1 and no constraints on the solar capacity.

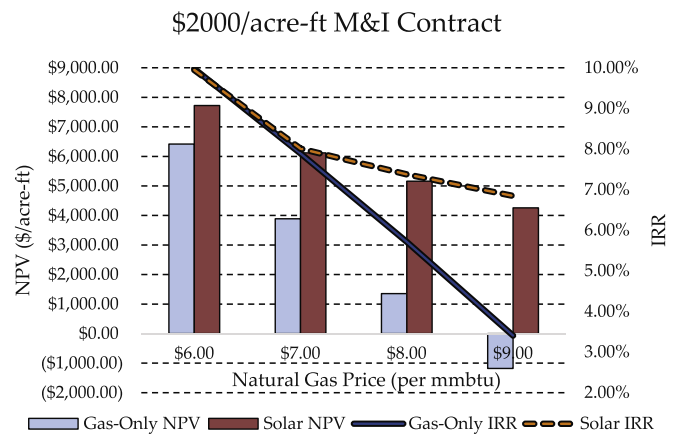


Fig. 3. The economic summary of the desalination projects with and without solar considering \$2000/acre-ft M&I water contract pricing at Year 1 and no constraints on the solar capacity.

As previously mentioned, the sensitivity of the NPV to the cost of capital (debt financing rate) was also considered. Similar to the effects of the water contract price on the NPV, the financing rate only impacted the optimal NPV and not the optimal design. Further, the magnitude of the impact of the financing rate has on

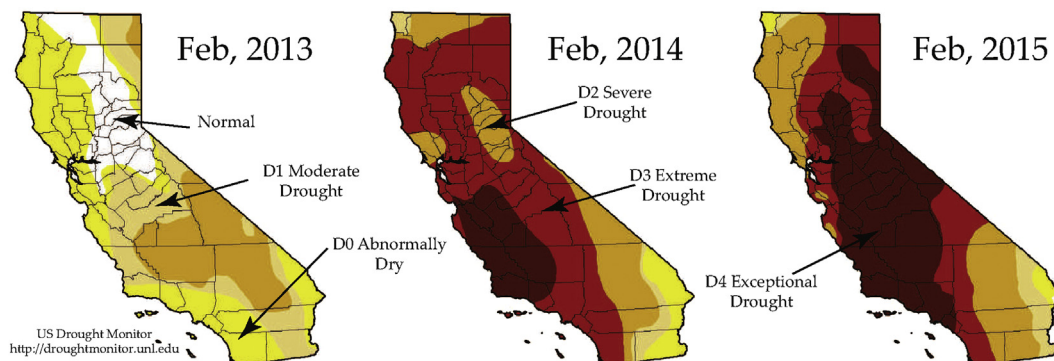
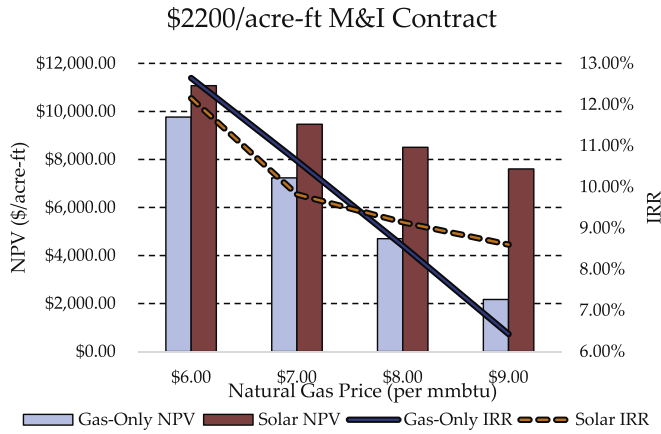


Fig. 1. The distribution of water scarcity across the State of California from February 2013 (left) to February 2015 (right) [5].



**Fig. 4.** The economic summary of the desalination projects with and without solar considering \$2200/acre-ft M&I water contract pricing at Year 1 and no constraints on the solar capacity.

the project NPV is independent of the water contract price but quite dependent on the natural gas price. This is expected since the contract price does not change the optimal design; however, the natural gas price does. Lastly, since the gas-only system design is static, so is the impact of the financing rate on the project NPV. Table 2 shows how the solar project NPV changes as the cost of capital is increased from 4% to both 5% and 6%. As can be seen, raising the cost of capital may have serious impacts on the economic viability of the project. For instance, if the cost of capital were 6%, a water contract price of \$1800/acre-ft would yield a negative NPV with \$9/mmbtu natural gas pricing, holding all other parameters constant. It's worth noting that although raising the cost of capital has less of an impact on the gas-only NPV—which is intuitive since the capital investment is lower—the solar project is still economically favored for each natural gas price and water contract price.

3.2. Solar array modeling

The results from the solar array and storage model are summarized in Fig. 5 for each optimal design in Table 1. The Thermal Load is the amount of thermal energy required by the desalination process to operate. The Usable Solar Energy is the actual amount of thermal energy that the solar array and storage system are able to provide to the desalination process whereas the Total Solar Energy is the solar energy potential if the design was not limited by the storage capacity and/or the maximum thermal load. The difference between the total solar energy and the usable solar energy is the amount of solar thermal energy that is lost due to design constraints. The ratio of the usable solar energy to the thermal load is the monthly solar fraction and, of course, the weighted average of the monthly solar fractions is the yearly average solar fraction  $f_s$ .

For each of the optimal designs, there is very little solar energy loss which is indicative of a well-matched thermal storage

**Table 2**

The change in the solar project NPV by increasing the cost of capital (debt financing rate) from the original value of 4% for each of the optimal designs corresponding to the natural gas prices.

Cost of capital	\$6.00/mmbtu	\$7.00/mmbtu	\$8.00/mmbtu	\$9.00/mmbtu
5%	\$-416.30	\$-477.01	\$-530.60	\$-540.97
6%	\$-834.94	\$-934.71	\$-1076.00	\$-1096.97

system to the solar array. It is worth noting that attempting to capture 100% of the total solar energy is a futile exercise that requires a theoretical infinite-capacity thermal storage system in the general case. For example, the optimal solution for the \$9/mmbtu shows that the theoretical maximum solar fraction, defined as the ratio of the yearly total solar energy to yearly total thermal load, is 69%. The optimal design yields a yearly average solar fraction of 65.07%; a difference of about 4 percentage points. By doubling the thermal storage capacity to 22.3h, the yearly average solar fraction only increases to 66.43%. However, the NPV takes a substantial hit dropping by 200% of its original value. This result further reinforces the need for the techno-economic analysis and optimization framework, presented herein, at the design stage.

3.3. Robust design

The robust design problem (4) was successfully solved and the analysis of each subproblem ensured that the optimal solution is very near a global optimum. The SIP algorithm terminated after the lower-level program furnished a SIP-feasible point. The optimal solution verified that the previous hypothesis of the worst-case was the \$9/mmbtu and \$1800/acre-ft scenario for which the optimal design favored a 65.07% solar fraction resulting from 36 solar collectors per module and 11.14h of thermal storage. The worst-case project NPV was verified to be \$909.18 per acre-ft/yr capacity. This result is quite striking when comparing with the non-renewable case. For the non-renewable case, the NPV is roughly \$-4500 per acre-ft/yr which strongly suggests that even the case of “doing nothing” is economically favored over non-renewable desalination. Obviously, the non-renewable design option is not robust to uncertainty in natural gas prices and therefore is not a viable option to contribute to the long-term sustainability of the agribusiness.

3.4. An emphasis on solar

Each of the optimal designs identified in this study for the solar desalination case favored some fraction of solar over the gas-only alternative. However, for each water contract price considered, gas prices of \$6/mmbtu yielded an optimal solar fraction (i.e., the fraction of energy that the plant consumes that is supplied by solar) of just 30.15%. If we impose the constraint discussed previously, that at least 50% of the energy must come from solar, then the optimal solutions for \$6/mmbtu natural gas price look a bit different. For each contract price, the optimal

**Table 1**

The optimal design values and corresponding solar fractions for the range of natural gas prices.

Natural Gas price	\$6.00/mmbtu	\$7.00/mmbtu	\$8.00/mmbtu	\$9.00/mmbtu
$H^*$	0.2828	9.4665	10.8676	11.1408
$N_s^*$	16	31	34	36
$f_s^*$	30.15%	58.09%	62.91%	65.07%

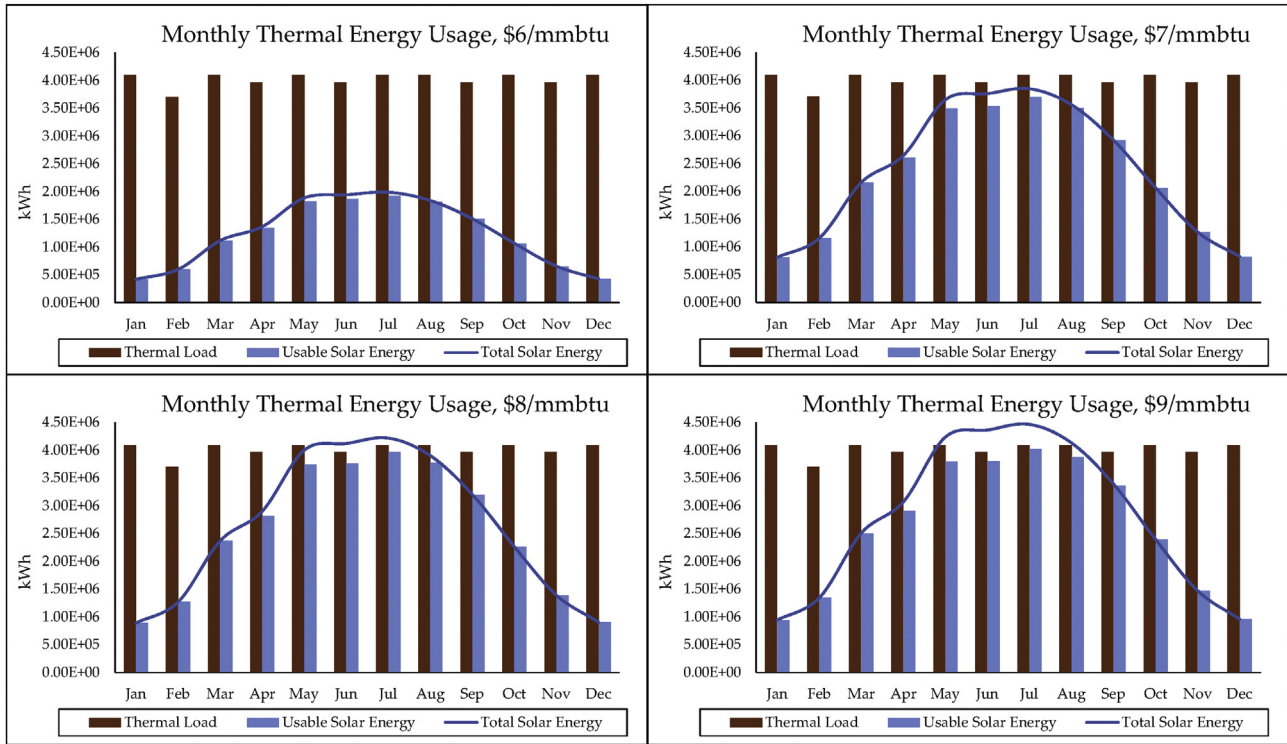


Fig. 5. The performance results of the solar model for the agricultural region in terms of total monthly thermal energy production per water treatment module versus the total thermal energy load of the process.

**Table 3**  
The differences between the unconstrained design case (no imposed emphasis on solar) and the constrained case (at least 50% of the energy must come from solar).

M&I price	Unconstrained NPV	Constrained NPV	Relative difference	Unconstrained IRR	Constrained IRR	Relative difference
\$1800/acre-ft	\$4376.14	\$4021.48	-8.10%	7.67%	6.98%	-8.89%
\$2000/acre-ft	\$7724.26	\$7369.60	-4.59%	9.95%	8.95%	-10.08%
\$2200/acre-ft	\$11,072.38	\$10,717.72	-3.20%	12.16%	10.84%	-10.81%

solutions for the constrained case yields a solar fraction of 50.15%. Table 3 contains the optimal solutions for both the constrained and unconstrained cases for comparison. As expected, in each case the constraint that at least a 50% solar fraction is required yields an optimal solution value (NPV) that is lower

than the unconstrained case. It is important to remind the reader that there was no value/cost placed on carbon emissions and so this reduction in value is essentially the result of placing a non-economic value on carbon emissions. If a monetary value or cost were placed on carbon emissions, say by tax or cap and trade, the

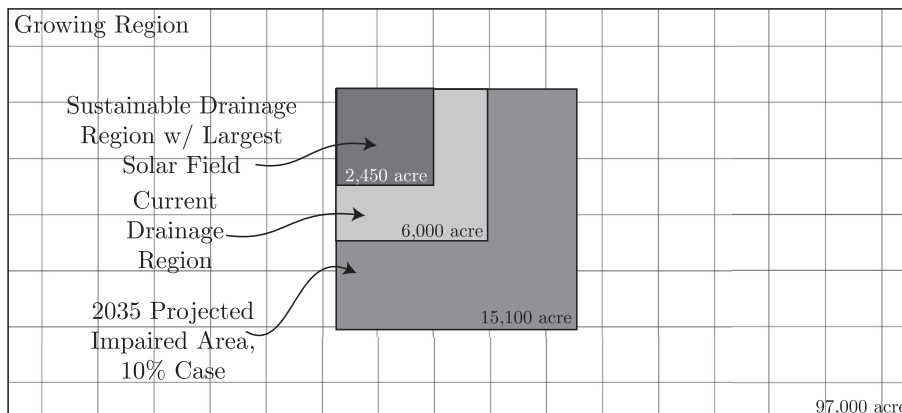


Fig. 6. The land-use for the current case study.

**Table 4**

The optimal design values and corresponding solar fractions for the range of natural gas prices for the case of growing almonds in the Central Valley.

Natural Gas price	\$6.00/mmbtu	\$7.00/mmbtu	\$8.00/mmbtu	\$9.00/mmbtu
$H^*$	0.0582	3.6900	10.8676	11.1145
$N_s^*$	15	22	34	35
$f_s^*$	28.49%	41.38%	62.91%	64.13%

solutions here are expected to change dramatically. Essentially, costs from carbon would effectively be reflected as higher natural gas costs which, as can be seen from Fig. 2 through Fig. 4, begin to strongly favor greater solar fractions.

### 3.5. Sustainability and land-use

In Fig. 6, the agricultural land-use is visualized comparing the current situation to the future projections with and without desalination. The 2035 projected impaired area, following from the retirement of 10% of the growing region, represents a growth of impaired area of 152%. Further, without a long-term solution, the impaired region will continue to grow. However, with solar desalination, the impaired region (and region occupied by the solar array and water treatment plants) will reduce the current drainage region area by nearly 60% returning 3550 acres of land back to primary growing region at the start of the project and saving an additional 9100 acres of land by year 2035.

### 3.6. Broad implications and region-wide projections

Throughout the drainage-impaired regions in the Central Valley, these results have broad implications. As indicated in the Introduction Section 1.2, the drainage impaired and salt impaired regions are vast, especially on the west side of the San Joaquin Valley. The results of this study translate to regions beyond the 97,000 acres originally considered, and directly scale provided the assumptions continue to hold true. This is because the NPV of the project is calculated on the basis of acre-ft of water produced annually. Given similar solar resource conditions across the Central Valley, the optimal solar footprints determined will also scale directly. Considering only the 379,000 acres of impaired land estimated in Section 1.2, it is estimated that over 1 million acre-ft per year of agricultural drainage is available for treatment.

The economic argument for solar desalination is made even stronger when considering the land value both with and without irrigation (aside from crop revenues). In the case where land is retired due to being salt impaired and/or drainage impaired, it has essentially lost its entire value—except perhaps as a drainage sink—both from lost crop revenues as well as future revenues. With region-wide drainage and salinity management via desalination, this scenario can be avoided; ensuring long-term sustainability.

The main case study presented above considered average crop revenues of \$2340/acre. This is fairly representative of general seed crop production value in Fresno County [35]. However, for a permanent crop such as almonds, the crop revenue can be much higher. For instance, average crop revenues from almonds in Fresno County in 2013 (the most current data) were \$6450/acre [35] with total revenues over \$1.1B. Furthermore, permanent crops are much more dependent on the long-term sustainability of soil health. Therefore, the consideration of permanent agriculture within this framework is quite relevant.

The parametric optimization formulation (2) was solved with the almond revenue for each natural gas price and water contract price as before. The optimal solutions are given in Table 4. The

optimal solutions for the almond case do not vary substantially from the results in Table 1. However, in each case besides the \$8/mmbtu natural gas price, a lower solar fraction is favored. This behavior is expected since the only change that was made placed a greater value on arable land. Hence, implementing desalination would be a more favorable value proposition; however, solar would appear to be less favorable without a value/cost placed on carbon emissions from natural gas. Despite the substantial increase in land value over the base case favoring less solar, solar thermal desalination for agricultural reuse is still an economically-favorable solution to the salt accumulation and sustainability problem in the region. That is, in each case, the solar thermal desalination project is economically favored over the gas-only desalination case, which in turn is favored over the “doing nothing” case.

## 4. Conclusion

In this paper, a case study was presented for a current agricultural region in California's Central Valley facing economic and environmental challenges stemming from historic unsustainable irrigation practices. Such practices have led to a net accumulation of salts in the soil which, when combined with a high water table, lead to impairment of otherwise-fertile land as well as contamination of groundwater and adverse effects on natural wildlife and habitat. Currently, the salinity of fertile soil is controlled through special drainage infrastructure whereby salty water is drained from the fields during irrigation and collected in a “drainage region” set aside for storing this water. Without a long-term solution for dealing with this water, the drainage region is projected to grow substantially as well as contaminate both surface water and groundwater resources.

This work builds upon the results of a novel solar thermal desalination technology piloted in the region in 2013–2014. Solar thermal desalination of agricultural drainage water is considered as one long-term solution to the growth of salt impaired lands in the region. A parabolic trough solar thermal concentrator technology coupled with limited-capacity thermal storage was modeled using solar resource data for the region. The optimal design of the solar system, used to power the thermal desalination process, was analyzed using both parametric optimization and robust design frameworks. In every case, the project economics favor implementing solar thermal desalination over the strategy of retiring land due to salt impairment. Further, in every case, the net-present value of the project favors some amount of CST to offset natural gas consumption. In the worst-cases of high natural gas costs and low water contract pricing, CST is the enabling technology for economic feasibility of thermal desalination in the region as well as long-term sustainability of regional agribusiness.

## Acknowledgment

Thank you to the folks at the Panoche Drainage District and Summers Engineering for helping retrieve data useful for this regional study.

## Appendix A

Table A1

The definition of the symbols used throughout this paper.

Definition of symbols	
$A_{PTC}$	Aperture area of a PTC, m <sup>2</sup>
$A_{rec}$	Land area recovered from drainage for growing, m <sup>2</sup>
$C_0$	Year 0 capital investment, \$
$C_{ag}$	Yearly revenue from agriculture, \$/acre
$C_e$	Cost of electricity, \$/kWh
$C_i$	Year $i$ cash flow, \$
$C_{i,AgR}$	Year $i$ profits from farming recovered drainage land, \$
$C_{i,cap}$	Year $i$ capital payment (debt service), \$
$C_{i,op}$	Year $i$ operating costs, \$
$C_{i,wat}$	Year $i$ revenues from water sales, \$
$C_{gas}$	Natural gas cost, \$/mmbtu
$C_{MED}$	Capital cost of MED train, \$
$C_{PTC}$	Capital cost of a single PTC, \$
$C_{ts}$	Capital cost of thermal storage, \$/kWh
$C_{water}$	Water contract price, \$/acre-ft
$\mathbf{d}$	Design variable vector for optimization, (–, h)
$D$	Design interval for optimization, (–, h)
$\hat{E}_e$	Specific electrical energy consumption, kWh/m <sup>3</sup>
$\hat{E}_t$	Specific thermal energy consumption, kWh/m <sup>3</sup>
$F_c$	Parameter (costs) interval set for optimization
$F_d$	Feasible design set
$f_{NPV}$	Net-present value function, \$/acre-ft-yr
$f_{NPV}^*$	Optimal net-present value function, \$/acre-ft-yr
$f_s$	Yearly average solar fraction, kWh solar/total kWh consumed
$f_s^*$	Yearly average solar fraction corresponding to the optimal design, kWh solar/total kWh consumed
$H$	Thermal storage capacity, h
$H^*$	Thermal storage capacity corresponding to the optimal design, h
LBD	Lower bound on optimal solution, –
$N_{MED}$	Number of MED trains, –
$N_s$	Number of PTCs, –
$N_s^*$	Number of PTCs corresponding to the optimal design, –
$\mathbf{p}$	Cost variable vector for optimization, (\$/acre-ft, \$/mmbtu)
$P$	Cost interval for optimization, (\$/acre-ft, \$/mmbtu)
$\dot{Q}$	Total thermal power required for desalination, kW
$r$	Optimization algorithm relaxation parameter, –
$r_c$	Cost of capital, financing APR, –
$r_d$	Capital discount rate, –
$r_{profit}$	Profit margin on agriculture, –
UBD	Upper bound on optimal solution, –
$V_w$	Freshwater production rate, acre-ft/yr
Greek Letters	
$\epsilon^{g,k}$	SIP algorithm restriction parameter, –
$\epsilon_{tol}$	SIP algorithm convergence tolerance, –
$\eta$	Robust design variable, –
$\rho_{PTC}$	Packing density of PTCs, m <sup>2</sup> aperture/m <sup>2</sup> footprint

## A.1. Optimization model

The annual average direct normal irradiance (DNI) for the

**Table A2**  
The annual average DNI (kWh/m<sup>2</sup>/day) for the location as broken down by month [22].

Jan	2.56
Feb	3.87
Mar	5.44
Apr	6.53
May	7.67
Jun	8.58
Jul	8.55
Aug	8.14
Sep	7.20
Oct	5.81
Nov	3.99
Dec	2.93
Ann. Avg	5.95

agricultural region considered herein is shown in Table A2 as broken down by month. The parameters used in modeling the PTC are given in Table A3.

Table A3

The parameters used in modeling the solar array.

Mirror reflectance	0.935
Glass receiver cover transmittance	0.963
Absorptance of receiver glass	0.96
HCE shadowing factor	0.98
Tracking error	0.994
Geometry error	0.98
Generic losses	0.96
Mirror reflectivity	0.88
Aperture length	6m
Rim angle	90°
Mirror length	109.33m
Absorber tube OD	0.05m

## A.2. Robust Optimization

The project NPV is calculated using the following expression

$$V_w f_{\text{NPV}}(N_s, H, C_{\text{water}}, C_{\text{gas}}) = \sum_{i=1}^{20} \frac{C_i(N_s, H, C_{\text{water}}, C_{\text{gas}})}{(1+r_d)^i} - C_0 \quad (\text{A.1})$$

with Year  $i$  cash flows,  $C_i$ , calculated as:

$$C_i(N_s, H, C_{\text{water}}, C_{\text{gas}}) = C_{i,\text{AgR}} + C_{i,\text{wat}} - C_{i,\text{cap}} - C_{i,\text{op}} \quad (\text{A.2})$$

The revenue from the water sales is constant for a given value of  $C_{\text{water}}$  but the profits from farming the recovered drainage land, the capital costs, and the operating costs are all dependent on the final design (as well as the contract water price and natural gas price). The capital cost is calculated by amortizing the total Year 0 capital investment,  $C_0$ , over 10 years with interest compounded monthly:

$$C_{i,\text{cap}} = r_c C_0 \left(1 + \frac{r_c}{12}\right)^{120} \left( \left(1 + \frac{r_c}{12}\right)^{120} - 1 \right)^{-1} \quad (\text{A.3})$$

The Year 0 capital investment is calculated as

$$C_0 = N_s C_{\text{PTC}} + \dot{Q} H C_{\text{ts}} + N_{\text{MED}} C_{\text{MED}} \quad (\text{A.4})$$

The revenue from water sales is given by

$$C_{i,\text{wat}} = V_w C_{\text{water}} \quad (\text{A.5})$$

The operating costs are given by

$$C_{i,\text{op}} = \left( \hat{E}_e C_e + \frac{\hat{E}_t C_{\text{gas}}}{293.1 \text{ kWh/mmBtu}} (1 - f_s) \right) V_w (1233.5 \text{ m}^3/\text{acre} - \text{ft}) \quad (\text{A.6})$$

The yearly average solar fraction  $f_s$  is determined from the detailed (8760 h/yr) modeling of the solar array and is therefore a function of the design variables ( $N_s, H$ ). Finally, the profit from farming drainage land is given by

$$C_{i,\text{AgR}} = A_{\text{rec}} C_{\text{ag}} r_{\text{profit}} \quad (\text{A.7})$$

where the land recovered from drainage at Year  $i$  is given by

$$A_{\text{rec}} = (6000 + 455i) \text{ acre} - (2100 \text{ acre} + N_s A_{\text{PTC}} / \rho_{\text{PTC}}) \quad (\text{A.8})$$

### A.3. Robust optimization

In this section, the algorithm for identifying a solution of (4) is discussed. In order to solve (4), it is first reformulated as the equivalent semi-infinite program:

$$\eta^* = \min_{\mathbf{p} \in P, \eta \in \mathbb{R}} \eta \quad (\text{A.9})$$

s.t.  $f_{\text{NPV}}(\mathbf{p}, \mathbf{d}) - \eta \leq 0, \forall \mathbf{d} \in D$

where  $\mathbf{p} = (C_{\text{water}}, C_{\text{gas}})$  and  $\mathbf{d} = (N_s, H)$  with  $P = [1800, 2200] \times [6, 9]$  and  $D = [13, 52] \times [0, 12]$  as compact intervals. Since (4) is equivalent to (A.9), solving (A.9) yields a solution of (4).

The robust optimization algorithm used to solve (A.9) relies on solving three nonlinear optimization subproblems. The three nonlinear programming (NLP) subproblems are formulated below.

#### A.3.1. Lower-Bounding Problem

$$\eta^{\text{LBP}} = \min_{\mathbf{p} \in P, \eta \in \mathbb{R}} \eta \quad (\text{A.10})$$

s.t.  $f_{\text{NPV}}(\mathbf{p}, \mathbf{d}) - \eta \leq 0, \forall \mathbf{d} \in D^{\text{LBP}}$

where  $D^{\text{LBP}} \subset D$  is a finite set.

#### A.3.2. Inner Program

$$\bar{\gamma}(\bar{\mathbf{p}}, \bar{\eta}) = \max_{\mathbf{d} \in D} [f_{\text{NPV}}(\bar{\mathbf{p}}, \mathbf{d}) - \bar{\eta}] \quad (\text{A.11})$$

If  $\bar{\gamma}(\bar{\mathbf{p}}, \bar{\eta}) \leq 0$ , then  $(\bar{\mathbf{p}}, \bar{\eta})$  is an SIP-feasible point.

#### A.3.3. Upper-bounding problem

$$\eta^{\text{UBP}} = \min_{\mathbf{p} \in P, \eta \in \mathbb{R}} \eta \quad (\text{A.12})$$

s.t.  $f_{\text{NPV}}(\mathbf{p}, \mathbf{d}) - \eta \leq -\varepsilon^{\text{g},k}, \forall \mathbf{d} \in D^{\text{UBP}}$

where  $D^{\text{UBP}} \subset D$  is a finite set and  $\varepsilon^{\text{g},k} \in \mathbb{R}$  with  $\varepsilon^{\text{g},0} > 0$ .

#### A.3.4. Algorithm

The algorithm presented here comes from Refs. [29,32] with changes in notation relevant for this application.

##### Algorithm A.1.

1. (Initialization)
  - (a) Set  $\text{LBD} := -\infty, \text{UBD} := +\infty, \varepsilon_{\text{tol}} > 0, k := 0$ .
  - (b) Set initial design sets  $D^{\text{LBP}} := D^{\text{LBP},0}, D^{\text{UBP}} := D^{\text{UBP},0}$ .
  - (c) Set  $\varepsilon^{\text{g},0} > 0$  and  $r > 1$ .
2. (Termination) Check.  $\text{UBD} - \text{LBD} \leq \varepsilon_{\text{tol}}$ .
  - (a) If true,  $\eta^* := \text{UBD}$ , terminate.
  - (b) Else,  $k := k + 1$ .
3. (Lower-Bounding Problem) Solve (A.10) to global optimality.
  - (a) Set  $\text{LBD} := \eta^{\text{LBP}}$  and set  $(\bar{\mathbf{p}}, \bar{\eta})$  equal to the optimal solution found.
4. (Inner Program) Solve (A.11) to global optimality.
  - (a) If  $\bar{\gamma}(\bar{\mathbf{p}}, \bar{\eta}) \leq 0$ , set  $\mathbf{p}^* := \bar{\mathbf{p}}, \eta^* := \bar{\eta}$ , terminate algorithm.
  - (b) Else, add the optimal solution  $\bar{\mathbf{d}}$  to  $D^{\text{LBP}}$ .
5. (Upper-Bounding Problem) Solve (A.12) to global optimality.
  - (a) If feasible:
    - i. Set  $(\bar{\mathbf{p}}, \bar{\eta})$  equal to the optimal solution found and solve (A.11) to global optimality.
    - ii. If  $\bar{\gamma}(\bar{\mathbf{p}}, \bar{\eta}) < 0$ :
      - A. If  $\bar{\eta} \leq \text{UBD}$ , set  $\text{UBD} := \bar{\eta}, \mathbf{p}^* := \bar{\mathbf{p}}$ .
      - B. Set  $\varepsilon^{\text{g},k+1} := \varepsilon^{\text{g},k}/r$ , go to 2.
    - iii. Else ( $\bar{\gamma}(\bar{\mathbf{p}}, \bar{\eta}) \geq 0$ ), add the optimal solution  $\bar{\mathbf{d}}$  to  $D^{\text{UBP}}$ , go to 2.
  - (b) Else (infeasible), set  $\varepsilon^{\text{g},k+1} := \varepsilon^{\text{g},k}/r$ , go to 2.

The flowchart for Algorithm A.1 is shown in Fig. 7.

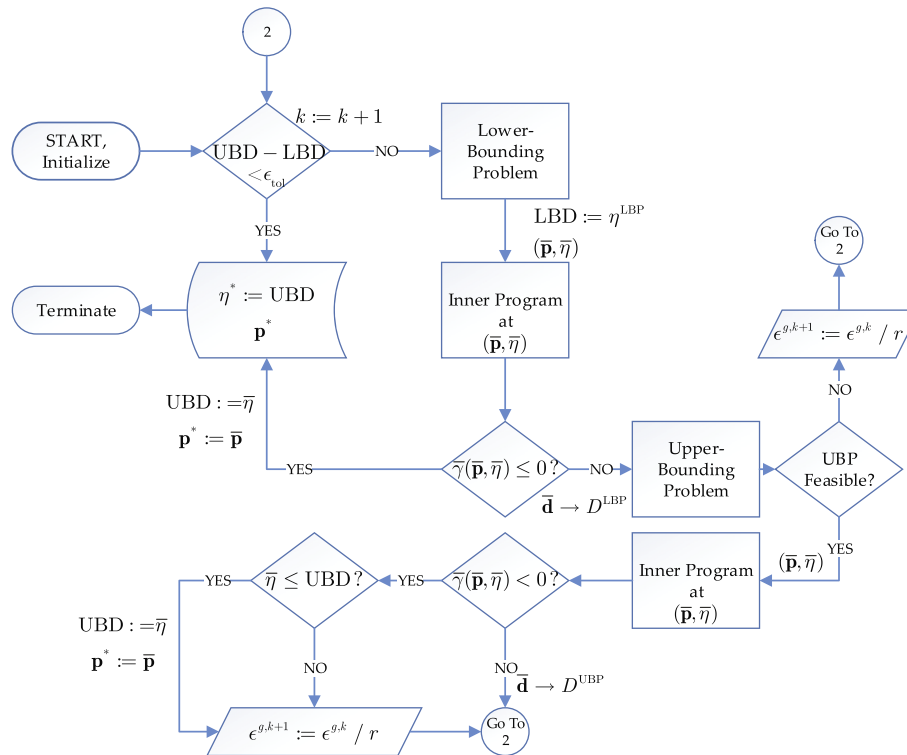


Fig. 7. The flowchart for the SIP Algorithm A.1.

## References

- [1] D. Griffin, K.J. Anchukaitis, How unusual is the 2012–2014 California drought? *Geophys. Res. Lett.* 41 (24) (2014) 9017–9023, <http://dx.doi.org/10.1080/02331934.2010.527970>.
- [2] N.S. Diffenbaugh, D.L. Swain, D. Touma, Anthropogenic warming has increased drought risk in California, *Proc. Natl. Acad. Sci.* 112 (13) (2015) 3931–3936, <http://dx.doi.org/10.1073/pnas.1422385112>.
- [3] D.W.R. California, California Agricultural Water Use, <http://www.water.ca.gov/wateruseefficiency/agricultural>, 2014 (accessed April 2014).
- [4] CA Dept of Food and Agriculture, California agricultural Statistics Review, 2013–2014, Tech. rep., CA Department of Food and Agriculture, 2014.
- [5] National Drought Mitigation Center, U. S. drought monitor (2015) (accessed 02/23/2015), <http://droughtmonitor.unl.edu/>.
- [6] R. Howitt, J. Medellín-Azuara, D. MacEwan, J. Lund, D. Sumner, Economic Analysis of the 2014 Drought for California Agriculture, Tech. rep., UC–Davis Center for Watershed Sciences, 2014 [https://watershed.ucdavis.edu/files/biblio/DroughtReport\\_23July2014\\_0.pdf](https://watershed.ucdavis.edu/files/biblio/DroughtReport_23July2014_0.pdf).
- [7] R. Valdmanis, Harvard buys up water rights in drought-hit wine country, Online (accessed 01/22/2015), <http://www.reuters.com/article/2015/01/22/us-harvard-water-idUSKBN0KV29G20150122>, January 2015.
- [8] Central Valley Regional Water QC Board, Salinity in the Central Valley, Tech. rep., Central Valley Regional Water QC Board, 2006.
- [9] N.W. Quinn, The San Joaquin Valley: Salinity and Drainage Problems and the Framework for a Response, in: D.B. Chang, A.C. Silva (Eds.), *Salinity and Drainage in San Joaquin Valley*, Springer, California, 2014, pp. 47–97.
- [10] Water Facts: Salt Balance in the San Joaquin Valley, [http://www.water.ca.gov/pubs/environment/salt\\_balance\\_in\\_the\\_san\\_joaquin\\_valley\\_water\\_facts\\_20\\_water\\_facts\\_20.pdf](http://www.water.ca.gov/pubs/environment/salt_balance_in_the_san_joaquin_valley_water_facts_20_water_facts_20.pdf), January 2001.
- [11] R. Howitt, J. Kaplan, D. Larson, D. MacEwan, J. Medellín-Azuara, G. Horner, et al., The Economic Impacts of Central Valley Salinity, Tech. rep., University of California Davis, 2009 [http://www.waterboards.ca.gov/rwqcb5/water\\_issues/salinity/library\\_reports\\_programs/econ\\_rpt\\_final.pdf](http://www.waterboards.ca.gov/rwqcb5/water_issues/salinity/library_reports_programs/econ_rpt_final.pdf).
- [12] B.C. McCool, A. Rahardianto, J. Faria, K. Kovac, D. Lara, Y. Cohen, Feasibility of reverse osmosis desalination of brackish agricultural drainage water in the San Joaquin Valley, *Desalination* 261 (2010) 240–250, <http://dx.doi.org/10.1016/j.desal.2010.05.031>.
- [13] J. Thompson, A. Rahardianto, H. Gu, M. Uchymiak, A. Bartman, M. Hedrick, et al., Rapid field assessment of RO desalination of brackish agricultural drainage water, *Water Res.* 47 (8) (2013) 2649–2660, <http://dx.doi.org/10.1016/j.watres.2013.02.013>.
- [14] Y. Cohen, B. McCool, A. Rahardianto, M.-m. Kim, J. Faria, Membrane Desalination of Agricultural Drainage Water, in: D.B. Chang, A.C. Silva (Eds.), *Salinity and Drainage in San Joaquin Valley*, Springer, California, 2014, pp. 303–341.
- [15] M.D. Stuber, C. Sullivan, S.A. Kirk, J.A. Farrand, P.V. Schillaci, B.D. Fojtasek, et al., Pilot demonstration of concentrated solar-powered desalination of subsurface agricultural drainage water and other brackish groundwater sources, *Desalination* 355 (2015) 186–196, <http://dx.doi.org/10.1016/j.desal.2014.10.037>.
- [16] J.D. Oster, D. Wichelns, E.W. Hilgard and the History of Irrigation in the San Joaquin Valley: Stunning Productivity, Slowly Undone by Inadequate Drainage, in: D.B. Chang, A.C. Silva (Eds.), *Salinity and Drainage in San Joaquin Valley*, Springer, California, 2014, pp. 7–46.
- [17] K.C. Knapp, K. Schwabe, K.A. Baerenklau, Regional Economics and Management in Closed Drainage Basins, in: *Salinity and Drainage in San Joaquin Valley*, Springer, California, 2014, pp. 353–379.
- [18] US Bureau of Reclamation, Water supply and yield study, Reclamation: Managing Water in the West, Technical Report.
- [19] S.A. Kalogirou, *Solar Energy Engineering Processes and Systems*, second ed., Academic Press, Oxford, 2014.
- [20] S. Gunasekaran, N. Mancini, R. El-Khaja, E. Sheu, A. Mitsos, Solar-geothermal hybridization of advanced zero emissions power cycle, *Energy* 65 (2014) 152–165, <http://dx.doi.org/10.1016/j.energy.2013.12.021>.
- [21] H. Ghasemi, E. Sheu, A. Tizzanini, M. Paci, A. Mitsos, Hybrid solar-geothermal power generation: optimal retrofitting, *Appl. Energy* 131 (2014) 158–170, <http://dx.doi.org/10.1016/j.apenergy.2014.06.010>.
- [22] National Renewable Energy Laboratory, Solar prospector, solar resource database, website. URL <http://maps.nrel.gov/prospector>.
- [23] R. A. Hoppe, D. E. Banker, Structure and finances of US farms, USDA-ERS Economic Information Bulletin 24.
- [24] A. Ghoheity, A. Mitsos, Optimal design and operation of a solar energy receiver and storage, *J. Sol. Energy Eng.* 134 (3) (2012) 031005, <http://dx.doi.org/10.1115/1.4006402>.
- [25] K.P. Halemane, I.E. Grossmann, Optimal process design under uncertainty, *AIChE J.* 29 (3) (1983) 425–433, <http://dx.doi.org/10.1002/aic.690290312>.
- [26] R.E. Swaney, I.E. Grossmann, An index for operational flexibility in chemical process design. Part I formulation theory, *AIChE J.* 31 (4) (1985) 621–630,

- <http://dx.doi.org/10.1002/aic.690310412>.
- [27] G. Ostrovsky, Y.M. Volin, E. Barit, M. Senyavin, Flexibility analysis and optimization of chemical plants with uncertain parameters, *Comput. Chem. Eng.* 18 (8) (1994) 755–767, [http://dx.doi.org/10.1016/0098-1354\(93\)E0013-Y](http://dx.doi.org/10.1016/0098-1354(93)E0013-Y).
- [28] M.D. Stuber, P.I. Barton, Robust simulation and design using semi-infinite programs with implicit functions, *Int. J. Reliab. Saf.* 5 (3) (2011) 378–397, <http://dx.doi.org/10.1504/IJRS.2011.041186>.
- [29] M.D. Stuber, A. Wechsung, A. Sundaramoorthy, P.I. Barton, Worst-case design of subsea production facilities using semi-infinite programming, *AIChE J.* 60 (7) (2014) 2513–2524, <http://dx.doi.org/10.1002/aic.14447>.
- [30] B. Kwak, E. Haug Jr., Optimum design in the presence of parametric uncertainty, *J. Optim. Theory Appl.* 19 (4) (1976) 527–546, <http://dx.doi.org/10.1007/BF00934653>.
- [31] J.E. Falk, K. Hoffman, A nonconvex max–min problem, *Nav. Res. Logist. Q.* 24 (3) (1977) 441–450, <http://dx.doi.org/10.1002/nav.3800240307>.
- [32] M.D. Stuber, P.I. Barton, Semi-infinite optimization with implicit functions, *Ind. Eng. Chem. Res.* 54 (2015) 307–317, <http://dx.doi.org/10.1021/ie5029123>.
- [33] A. Mitsos, Global optimization of semi-infinite programs via restriction of the right-hand side, *Optim* 60 (10–11) (2011) 1291–1308, <http://dx.doi.org/10.1080/02331934.2010.527970>.
- [34] Seawater desalination, The Carlsbad Desalination Project, Tech. rep., San Diego County Water Authority, July 2015 [http://www.sdcwa.org/sites/default/files/desal-carlsbad-fs-single\\_1.pdf](http://www.sdcwa.org/sites/default/files/desal-carlsbad-fs-single_1.pdf).
- [35] L. Wright, K. Ross, 2013 Fresno County Annual Crop and Livestock Report, Tech. rep., Fresno County Department of Agriculture, 2014.